Systems/Circuits

Independent Control of Presynaptic Inhibition by Reticulospinal and Sensory Inputs at Rest and during Rhythmic Activities in the Cat

Jennifer Sirois,[1] Alain Frigon,[2] and Jean-Pierre Gossard[1]

[1]Groupe de Recherche sur le Système Nerveux Central, Department of Physiology, Université de Montréal, Montreal, Quebec H3C 3J7, Canada, and
[2]Department of Physiology and Biophysics, Université de Sherbrooke, Sherbrooke, Quebec J1K 2R1, Canada

To be functionally relevant during movement, the transmission from primary afferents must be efficiently controlled by presynaptic inhibition. Sensory feedback, central pattern generators, and supraspinal structures can all evoke presynaptic inhibition, but we do not understand how these inputs interact during movement. Here, we investigated the convergence of inputs from the reticular formation and sensory afferents on presynaptic inhibitory pathways and their modulation at rest and during two fictive motor tasks (locomotion and scratch) in decerebrate cats. The amplitude of primary afferent depolarization (PAD), an estimate of presynaptic inhibition, was recorded in individual afferents with intra-axonal recordings and in a mix of afferents in lumbar dorsal rootlets (dorsal root potential [DRP]) with bipolar electrodes. There was no spatial facilitation between inputs from reticulospinal and sensory afferents with DRPs or PADs, indicating an absence of convergence. However, spatial facilitation could be observed by combining two sensory inputs, indicating that convergence was possible. Task-dependent changes in the amplitude of responses were similar for reticulospinal and sensory inputs, increasing during fictive locomotion and decreasing during fictive scratch. During fictive locomotion, DRP and PAD amplitudes evoked by reticulospinal inputs were increased during the flexion phase, whereas sensory-evoked DRPs and PADs showed maximal amplitude in either flexion or extension phases. During fictive scratch, the amplitudes of DRPs and PADs evoked by both sources were maximal in flexion. The absence of spatial facilitation and different phase-dependent modulation patterns during fictive locomotion are consistent with independent presynaptic inhibitory pathways for reticulospinal and sensory inputs.

Introduction

During movement, sensory feedback from the limbs must be filtered to be of functional relevance. An efficient way to gate sensory inflow in afferent terminals before it reaches spinal neurons is through presynaptic inhibition. Presynaptic inhibition, estimated from indirect measurements in human subjects, is often proposed as a mechanism to explain changes in the gain of reflex pathways during movement (Simonsen and Dyhre-Poulsen, 1999; Roche et al., 2011; Robertson et al., 2012), motor disorders (Calancie et al., 1993; Morita et al., 2000), and age or fatigue (Butchart et al., 1993). Presynaptic inhibition is produced by spinal interneurons with GABAergic axo-axonic synapses on primary afferent terminals (Eccles et al., 1962; Rudomin and

Schmidt, 1999; Hughes et al., 2005). With GABAergic activation, Cl⁻ anions escape the negative intra-axonal environment, thus producing a primary afferent depolarization (PAD) (Eccles et al., 1963; Nicoll and Alger, 1979; Cattaert and El Manira, 1999).

Presynaptic inhibition is not simply turned on whenever the motor pools are active, it is adjusted to task. For example, a sustained level of PAD is induced by stimulating the mesencephalon in decerebrate cats, but only if fictive locomotion is concomitantly evoked (Duenas and Rudomin, 1988; Perreault et al., 1999). In contrast, PAD amplitude evoked by sensory inputs is decreased during fictive scratch in decerebrate cats (Côté and Gossard, 2003). In humans, learning different precision grip tasks alters cervical spinal network excitability by modulating the level of presynaptic inhibition in IA afferents (Roche et al., 2011). Transmission in PAD pathways activated by sensory inputs is also modulated by the different phases of locomotion (Duenas and Rudomin, 1988; Gossard et al., 1989; Wolf and Burrows, 1995; Ménard et al., 1999).

It is known that supraspinal structures, including the sensorimotor cortex (Andersen et al., 1964; Meunier and Pierrot-Deseilligny, 1998), red nucleus (Hongo et al., 1972), vestibular nuclei (Cook et al., 1969), brainstem, and cerebellum (Carpenter et al., 1966), may evoke or inhibit PAD at rest. In anesthetized cats, Rudomin et al. (1983, 1986) estimated PAD amplitude in response to various combinations of supraspinal and peripheral inputs. Cutaneous and reticular formation stimuli were particu-

larly useful to classify PAD patterns. Based on their findings, interneuronal circuits were drawn showing sensory and several supraspinal inputs projecting on the same PAD pathways. Even though experiments were not designed to verify such convergence, it suggested that commands from the brain and sensory inputs were meeting at the spinal interneuronal level to control presynaptic inhibition.

PAD can thus be evoked by stimulating sensory inputs, supraspinal structures, or central pattern generators (CPGs) (Rudomin and Schmidt, 1999; Rossignol et al., 2006). However, how these systems interact during movement remains largely unknown. Is presynaptic inhibition mainly under the control of spinal cord networks or can it be selectively activated by descending supraspinal commands? How are these inputs modulated by CPG drive? In this study, we investigated the convergence of reticulospinal and sensory inputs on PAD interneurons at rest and evaluated patterns of task- and phase-dependent modulation of PAD evoked by these two inputs during fictive locomotion and scratch.

Materials and Methods

General procedure. Acute experiments were performed on 31 cats of either sex (2.6–5.0 kg). All procedures were in accordance with the Guide for Care and Use of Experimental Animals (Canada) and approved by the Ethics Committee of the Université de Montréal. The details of the preparation were delineated previously (Frigon and Gossard, 2010) and are summarized here. Before surgery, cats were injected with an analgesic (Anafen 2 mg/kg; subcutaneously) and premedicated (Atravet 0.1 mg/kg, glycopyrrolate 0.01 mg/kg, ketamine 10 mg/kg; i.m.). Cats were anesthetized using a mixture of oxygen nitrous oxide and isoflurane (2–4%, Abbott Laboratories) during the surgery.

After a craniotomy, the cortex and all tissue rostral to the colliculi and mammillary bodies were removed (i.e., a precollicular/premammillary decerebration) (Leblond et al., 2000; Frigon and Gossard, 2010). At this point, animals are considered to have complete lack of sentience. Anesthesia was discontinued, and animals were paralyzed by injecting pancuronium bromide (1 mg/kg; Sandoz Canada) supplemented every 45 min. Paralysis is required to remove movement-related sensory feedback to study the centrally generated pattern of scratching or locomotion (i.e., "fictive" rhythms) and to allow stable intracellular recordings. Immediately after this injection, the animals were artificially ventilated for the duration of the experiment. A lethal injection of pentobarbital anesthetic was administered at the conclusion of the experiment.

Nerve recording and stimulation. To monitor scratch or locomotor episodes, the electroneurography (ENG) of selected muscle nerves of the left hindlimb was recorded by dissecting and mounting the following nerves on bipolar silver chloride electrodes: posterior biceps–semitendinosus (PBSt), semimembranosus–anterior biceps (SmAB), lateral gastrocnemius-soleus (LGS), medial gastrocnemius (MG), plantaris (Pl), flexor hallucis longus and flexor digitorum longus (FDHL) together, tibialis anterior (TA), extensor digitorum longus (EDL), and sciatic (Sci). The sartorius (Sart) and quadriceps (Quad) nerves were mounted in cuff electrodes. The cutaneous nerves, caudal cutaneous sural (CCS) and superficial peroneal (SP), were mounted on bipolar electrodes, whereas the medial plantar nerve (MPL) was mounted in a cuff electrode. After a laminectomy exposing spinal segments L5-S1, the animals were transferred to a stereotaxic frame, and skin flaps surrounding the spinal cord and the hindlimb nerves were used to construct mineral oil pools. The cord dorsum potential (CDP) was recorded with a silver-chloride ball electrode, and stimulation intensity was expressed as multiples of the threshold (T) for the most excitable fibers in the nerve determined by the first negative deflection of the CDP. At rest or during episodes of fictive scratch or locomotion, selected nerves were stimulated with trains of 1–6 pulses at 200 Hz with intensities between 1.0 and 5.0T. In some cases (as in Brink et al., 1984), it was necessary to stimulate two or three peripheral nerves together to recruit interneurons and evoke a PAD in a particular axon. ENG was bandpass filtered (10 Hz-10 kHz) and

amplified (Neuralynx). Episodes of fictive rhythms were digitized on-line with interactive custom-made software (Spinal Cord Research Center, University of Manitoba, Winnipeg, Manitoba, Canada) or off-line from recordings on videotape (15 channels; Vetter 4000A; A.R. Vetter). Data were analyzed using the same custom-made software.

Dorsal root potentials (DRPs) were recorded from proximal stumps of cut dorsal rootlets from L7 with bipolar silver chloride electrodes (Dubuc et al., 1988; Gossard and Rossignol, 1990). DRP signals are illustrated with negativity upward to visualize the compound PAD from the numerous axons (e.g., see Fig. 2). Intra-axonal recordings of identified primary afferents in the dorsal columns (Gossard et al., 1989, 1990, 1991, 1996; Ménard et al., 1999; Côté and Gossard, 2003) were performed (L6-S1) with glass micropipettes filled with K^+-acetate (2 M). Identification of primary afferents included the following: (1) threshold for activation (<2.0T for Group I, 2.0–5.0T for Group II); and (2) the ability to follow electrical stimulation of a specific nerve at high frequency (>500 Hz) with a short and constant latency and the absence of a prepotential on the evoked spike. Reticulospinal fibers (RS) were stimulated (6 impulses of 0.2 ms at 200 or 300 Hz) with a fine tungsten electrode (5 MΩ) either at the level of the medial longitudinal fasciculus (MLF) (Floeter et al., 1993; Gossard et al., 1996; Leblond et al., 2000; Cabaj et al., 2006) or in the vicinity of the gigantocellular tegmental field of the reticular formation (Rudomin et al., 1983, 1986). The electrode was first positioned according to stereotaxic coordinates and then moved up or down by fractions of millimeters to find sites able to evoke short-latency CDPs at the lumbar levels and negative DRPs with minimal current (<200 µA). An electrolytic lesion (see Fig. 1C) was done in the first few experiments to ascertain the localization.

Fictive scratch and locomotion. To evoke scratch, a laminectomy was made at C1-C2; and after removing the dura, a small cotton ball soaked in D-tubocurarine (0.1%; Sigma) was applied topically on the dorsal spinal surface (Feldberg and Fleischhauer, 1960). Episodes of fictive scratch occurred spontaneously or were induced by manual stimulation of the left pinna (Deliagina et al., 1975; Côté and Gossard, 2003). Spontaneous fictive locomotion was frequently observed (>50%) after a precollicular/premammillary decerebration that could last for several minutes, or hours in some cases. Manually stimulating the neck region, perineum or pinna, or short series of electrical stimuli to the sciatic nerve were sometimes used to initiate episodes of fictive locomotion. Only episodes with vigorous and regular ENG bursts during locomotion or scratch were selected for analysis. Bouts of ENG signals with a complete absence of bursts were selected as rest episodes.

Data analysis. DRPs and PADs were evoked by stimulating reticulospinal tracts or peripheral nerves with trains of electrical stimuli given 2–4 times per seconds, fast enough to obtain an optimal number of responses during rhythmic episodes but slow enough to prevent responses from influencing each other (Floeter et al., 1993; Gossard et al., 1996). The peak amplitude of DRPs and PADs was measured off-line and averaged for episodes of rest, scratch, and locomotion to evaluate task dependency. Responses evoked during flexion and extension phases were separated and averaged to evaluate phase-dependent modulation.

The convergence of inputs on common PAD interneurones was tested by the technique of spatial facilitation using DRP and PAD recordings at rest (Brink et al., 1984). PADs were evoked by each input individually and then by the combined stimuli (RS + sensory or sensory + sensory). The algebraic sum of the averaged individual PADs was then subtracted from the PAD elicited by the combined stimuli. When the combined PAD (e.g., Fig. 2E, third trace "Comb") is larger than the summed PAD (e.g., Fig. 2E, fourth trace "Σ"), the difference (Fig. 2E, fifth trace "Diff") shows a positive deflection. From this, we can conclude that the inputs converge on common interneuronal population and activated previously subthreshold interneurons. When the responses add linearly so that there is no difference between the combined PAD and the summed PAD, the subtraction leads to a flat line (e.g., Fig. 2A–D, see fifth trace), indicating an absence of spatial facilitation and no convergence. The coupling intervals used were either zero or the peripheral stimulation was delayed in some cases (by 19–55 ms) so that the peak amplitude of PADs or DRPs evoked by the two inputs occurred at the same time.

Burst duration was defined as the time between burst onset and termination of activity from the raw ENG waveforms. Cycle period was defined as the time between successive flexor or extensor burst onsets. Because cycles vary in length, they were normalized to the same period of time so that both the start and end of the cycle lined up. The flexor phase was determined by the duration of bursts in a flexor nerve, whereas the extensor phase was determined by the duration of bursts in an extensor nerve. During fictive scratch, the brief bursts of hip, knee, or ankle extensor nerves do not fill the gap between flexor bursts. As such, the phase alternating with flexion was measured by the time between two flexor phases (Frigon et al., 2010). All PADs and DRPs occurring in a given phase were averaged over the entire locomotor or scratch episode. In Figures 6 and 7, phase plots of averaged amplitude of PAD and DRPs (Gossard, 1996; Ménard et al., 1999) were vertically aligned with the averaged rectified activities of a flexor and an extensor nerve to illustrate the cyclic modulation.

Statistical analysis. Statistical analyses were performed to determine differences in DRP and PAD amplitudes obtained during rest, locomotion, and scratch (task dependency). Values were always compared within the same rootlet or axon. Statistical analyses were also applied to determine differences in DRP and PAD amplitude obtained in different phases of the fictive scratch or locomotor cycles (phase dependency). The Kolmogorov-Smirnov-Liliefors test was used to compare the shape and location of the distribution of responses to a normal distribution. If the data were normally distributed, the parametric Student's t test was performed, whereas the nonparametric Mann–Whitney rank-sum test was otherwise used. Significance for all statistical tests was $p < 0.05$.

Results

The first objective of the study was to determine whether reticulospinal inputs and sensory feedback converge on common interneurons involved in presynaptic inhibition of primary afferents. The second and third objectives were to determine whether the control of presynaptic inhibition by reticulospinal and sensory inputs is modulated by task and by phase.

Figure 1 provides a summary of the experimental setup (Fig. 1A), the number of axons recorded intracellularly (Fig. 1B), and the brainstem areas stimulated to evoke reticulospinal inputs (Fig. 1C). The DRP was recorded from L7 dorsal rootlets in response to reticulospinal and/or sensory inputs in 154 trials of 31 cats. PADs evoked by reticulospinal and/or sensory inputs were recorded in 68 afferents of 17 cats. Mean conduction velocities were 76.5 ± 10.8, 61.0 ± 18.1, and 56.2 ± 14.0 m/s for muscle, cutaneous, and sciatic afferents, respectively (Fig. 1B). There were 26 afferents from muscle nerves with conduction velocities >75 m/s that can be considered Group I fibers (Matthews, 1972). Reticulospinal inputs were evoked by stimulating the MLF (10 cats) or within the reticular formation near the gigantocellular and magnocellular tegmental fields (15 cats, see Fig. 1C). The results were essentially the same for these two regions, so they were pooled for analysis. Reticulospinal stimulation evoked a PAD in 67 of 68 afferents; and in only one (a Group I from LGS muscle), it evoked a primary afferent hyperpolarization (PAH). Sensory- and reticulospinal-evoked PADs and DRPs were recorded during rest, fictive locomotion, and fictive scratch.

Spatial facilitation between sensory and reticulospinal inputs

The convergence of sensory and reticulospinal inputs onto common presynaptic inhibitory pathways was tested by spatial facilitation using 124 pairs of inputs with DRP ($n = 65$) and PAD ($n = 59$) recordings. In some cases, separate trials testing different coupling intervals and intensities were performed.

DRPs

We evaluated 47 combinations of reticulospinal and sensory nerve inputs with DRPs in 27 cats. All of the stimuli led to nega-
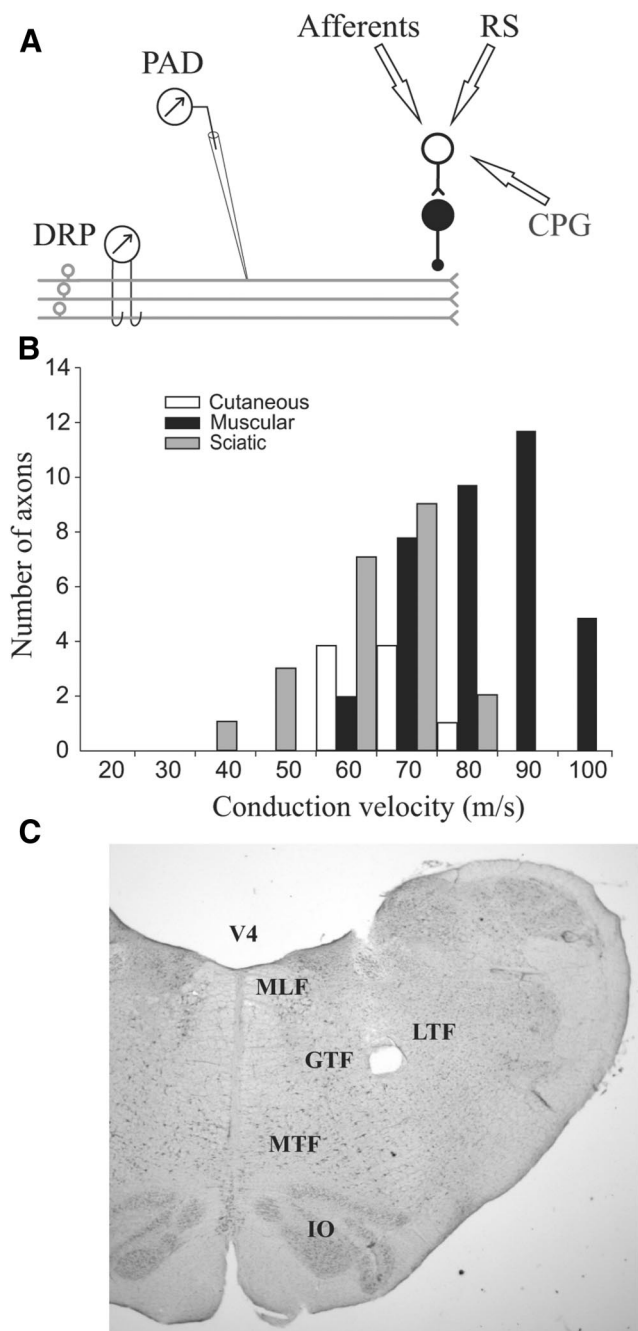

Figure 1. *A*, Schematic illustration of the recordings and PAD pathways. Top, Presynaptic inhibition is mediated by a chain of two spinal interneurons with an axo-axonic synapse on the afferent terminal. These interneurons are under the influence of three systems (arrows): sensory feedback from primary afferents, RS tracts, and CPGs. The evoked PAD is recorded intra-axonally with a micropipette or in many afferents from a dorsal rootlet as DRP. *B*, Distribution of the conduction velocities of the sample of primary afferents. Most afferents were Group I or II muscle afferents or large β cutaneous afferents. *C*, Photomicrograph of an electrolytic lesion (hole) near the gigantocellular tegmental field (GTF) in the brainstem. IO, Inferior olive; LTF, lateral tegmental field; MTF, magnocellular tegmental field; V4, fourth ventricle.

tive DRPs. Muscle afferent inputs ($n = 33$) were evoked by stimulating the PBSt ($n = 21$), Quad ($n = 3$), FDHL ($n = 3$), TA-EDL ($n = 2$), EDL ($n = 1$), GS-FDHL ($n = 1$), Pl-FDHL ($n = 1$), and Quad-FDHL ($n = 1$) nerves, whereas cutaneous afferent inputs ($n = 14$) were evoked by stimulating the SP ($n = 10$) and MPL ($n = 4$) nerves.

Figure 2*A–D* shows the absence of spatial facilitation between reticulospinal and muscle afferent inputs. For example, when reticulospinal inputs were combined with PBSt stimulation at delays of 0 ms (Fig. 2*A*) or 25 ms (Fig. 2*B*), the combined DRP was no different from the algebraic sum of the reticulospinal- and PBSt-evoked DRPs. A similar result was obtained when reticulospinal inputs were combined with another muscle afferent inputs (TA-EDL) at delays of 0 ms (Fig. 2*C*) or 20 ms (Fig. 2*D*).

Overall, there was an absence of spatial facilitation between reticulospinal and muscle afferent inputs in 31 of 33 trials (94%), as well as between reticulospinal and cutaneous afferent inputs in 14 of 14 trials (100%). Together, there was no facilitation between reticulospinal and sensory inputs in 45 of 47 trials (95.7%). In 21 trials (45% of trials) (11 with muscle afferents, 10 with cutaneous afferents), the spatial facilitation test led to a negative deflection, indicating that the combined stimuli evoked a smaller response than the sum of individual responses (see Discussion).

In some of the same dorsal rootlets as those used for evaluating convergence of reticulospinal and sensory inputs, we also tested spatial facilitation between two sensory inputs (Brink et al., 1984). Eighteen sensory combinations were done in 13 cats, including 15 between muscle afferents, 1 between muscle and cutaneous afferents, and 2 between cutaneous afferents. An example of spatial facilitation between muscle afferent inputs is shown in Figure 2*E*, *F*. When PBSt stimulation was combined with TA-EDL stimulation (delay of 0 ms), the combined DRP was larger than the algebraic sum of the individual DRPs with moderate intensity of stimulation recruiting most Group I afferents (Fig. 2*E*) or very low intensity of stimulation recruiting only the largest afferent fibers (Fig. 2*F*). Spatial facilitation between sensory inputs was observed in 4 of 18 trials (between Group I afferent inputs of PBSt and LGS, PBSt and Sart, and twice between PBSt and TA-EDL). Therefore, the experimental conditions were conducive to demonstrate spatial facilitation.

PAD

The DRP includes a mix of PADs from numerous axons that could display different levels of facilitation, or none at all. As a result, we also evaluated convergence in individual afferent axons using intracellular recordings. Overall, 59 combinations of reticulospinal and sensory inputs were tested in 50 axons of 15 cats. Muscle afferent inputs ($n = 54$) were evoked by stimulating the PBSt ($n = 34$), FDHL ($n = 12$), TA-EDL ($n = 4$), GS ($n = 1$), GS-FDHL ($n = 1$), Pl-FDHL ($n = 1$), and Quad-FDHL ($n = 1$)
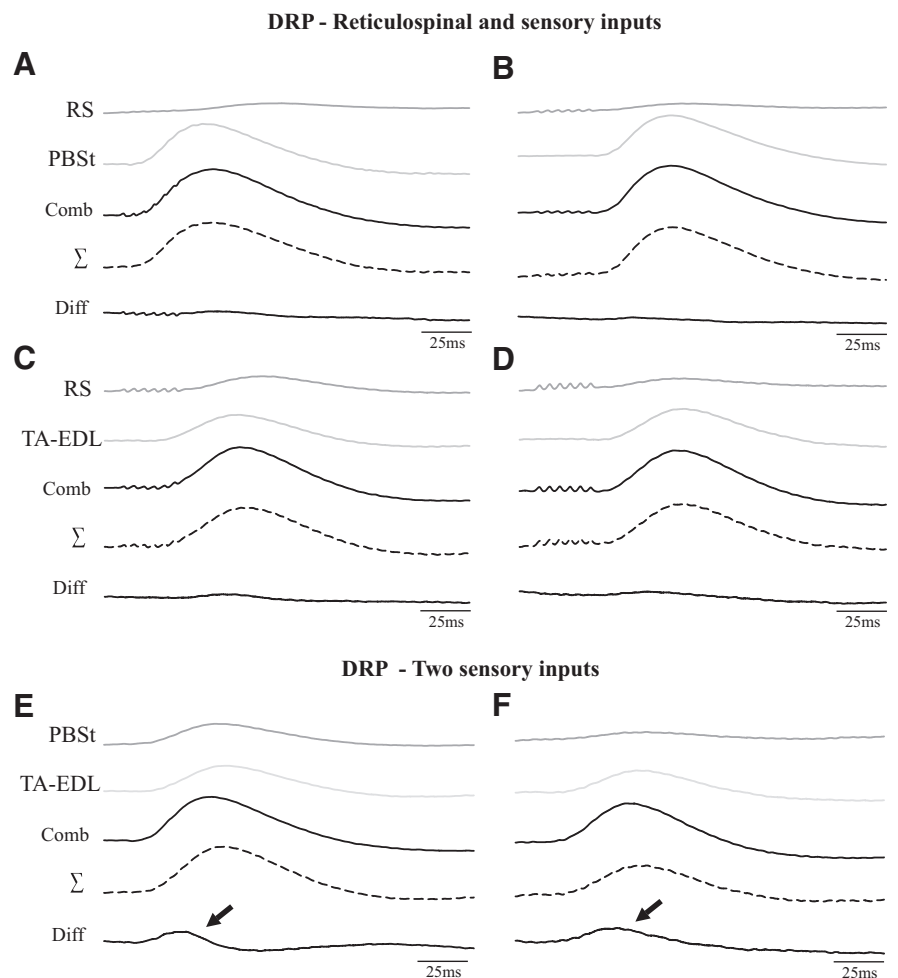
DRP - Reticulospinal and sensory inputs

DRP - Two sensory inputs

Figure 2. DRP: spatial facilitation. *A–F*, Top to bottom, The average DRP evoked by (1) one input (reticulospinal or sensory); (2) a second input (sensory); (3) the combined stimuli (synchronized or not); (4) the algebraic sum of individual DRPs (Σ); and (5) the result of subtracting the sum from the DRP evoked by combined inputs (Diff). *A*, The combined stimuli (interval 0 ms) of reticular formation (RS, 6p, 200 Hz, 150 μA) and of the PBSt (6p, 200 Hz, 2T) evoked a DRP that was not different from the summed DRPs. *B*, The PBSt input was delayed by 25 ms so that the peaks of DRPs occurred together, and the result is the same. *C*, The combined stimuli (interval 0 ms) of RS (6p, 200 Hz, 150 μA) and of the nerves to TA-EDL (6p, 200 Hz, 1.3T) evoked a DRP that that was not different from the summed DRPs. *D*, The TA-EDL stimuli were delayed by 20 ms so that the peaks of DRPs occurred together, and the result was the same. *E*, The combined sensory stimuli (interval 0 ms) of PBSt (6p, 200 Hz, 1.5T) and of TA-EDL (6p, 200 Hz, 1.3T) nerves evoked a DRP with larger amplitude than the algebraic sum (arrow). *F*, The same inputs were combined using a lower stimulation intensity for PBSt (6p, 200 Hz, 1.3T) and TA-EDL (6p, 200 Hz, 1.0T) nerves to reduce possible occlusion, and the DRP from the combined inputs was clearly larger than the summed DRPs (arrow). *A–F*, All traces are from the same L7 rootlet with the same amplification.

nerves, whereas cutaneous afferent inputs ($n = 6$) were evoked by stimulating the SP ($n = 5$) and MPL ($n = 1$) nerves.

Figure 3 shows the absence of spatial facilitation between reticulospinal and muscle afferent inputs in SmAB (Fig. 3*A*, *C*) and EDL (Fig. 3*E*) Group I axons. In all 3 examples shown, when reticulospinal inputs were combined with PBSt (Fig. 3*A*), GS (Fig. 3*C*), or FDHL (Fig. 3*E*) stimulation, the combined PAD was no different from the algebraic sum of the individual PADs. Overall, there was only 1 case of spatial facilitation between reticulospinal and SP inputs in an MG Group I afferent. Thus, there was a complete absence of facilitation between reticulospinal and muscle afferents (0 of 54) and only one case between reticulospinal and cutaneous afferent inputs (1 of 6).

Although spatial facilitation was absent in the 3 axons shown in Figure 3 when reticulospinal and muscle Group I afferent inputs were combined, spatial facilitation was found
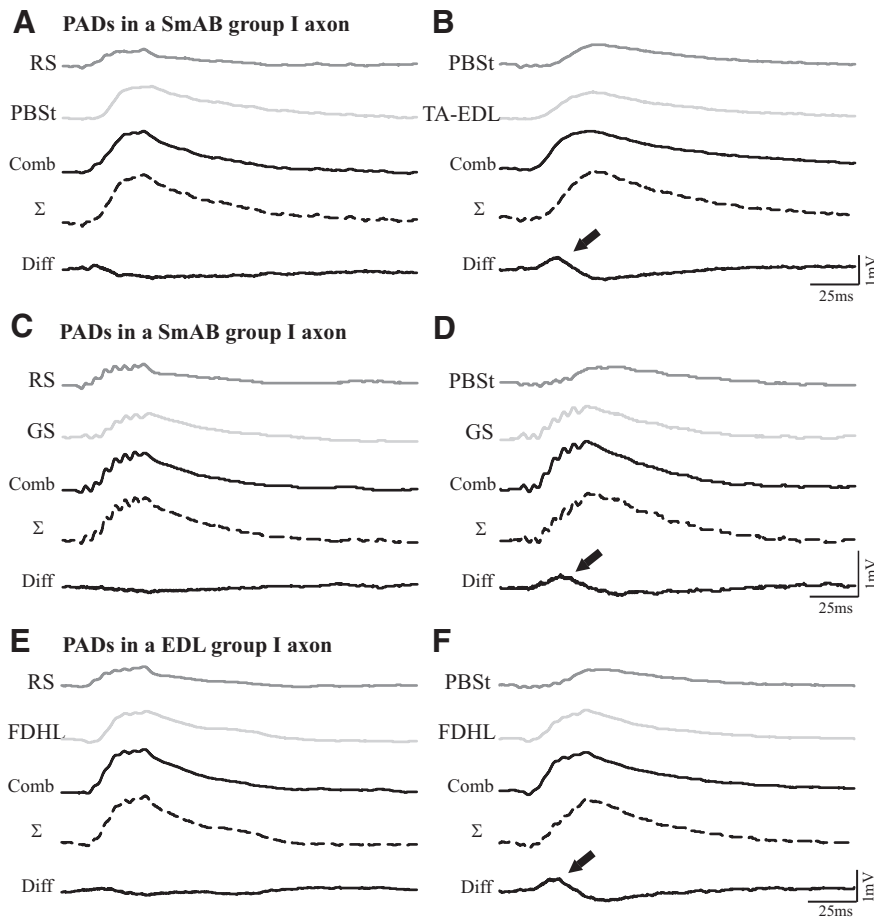
PAD - Reticulospinal and sensory inputs

Figure 3. PAD: spatial facilitation. Outline as in Figure 2. **A**, The combined stimuli of reticular formation (RS, 6p, 200 Hz, 150 μA) and of PBSt (6p, 200 Hz, 2T) evoked an average PAD, in a Group I axon from the SmAB muscle that was not different from the summed PADs. **B**, Two sensory nerves, PBSt (6p, 200 Hz, 2T) and TA-EDL (6p, 200 Hz, 2T), were stimulated individually and in combination in the same axon. The subtraction (Diff) showed a clear positivity (arrow). **C**, The combined stimuli of RS (6p, 200 Hz, 200 μA) and of GS (6p, 200 Hz, 2T) evoked an average PAD in another SmAB Group I axon that was not different from the summed PADs. **D**, Stimulating two sensory inputs, PBSt (6p, 200 Hz, 1.3T) and GS (6p, 200 Hz, 2T), evoked average PADs in the same axon. The PADs evoked by the combined stimuli were clearly larger (arrow) than the summed PADs. **E**, The combined stimuli of RS (6p, 200 Hz, 150 μA) and of FDHL (6p, 200 Hz, 2T) evoked an averaged PAD, in a Group I axon from EDL muscle, that was not different from the algebraic sum. **F**, Two sensory inputs, PBSt (6p, 200 Hz, 2T) and FDHL (6p, 200 Hz, 2T), were stimulated individually and in combination in the same axon, and the subtraction (Diff) showed a clear positivity (arrow).

when inputs from two muscle Group I afferents were combined (Fig. 3B,D,F). Overall, the spatial facilitation of two sensory inputs was tested using 14 combinations (all muscle afferents) in 14 axons to determine whether the conditions for convergence were present. Spatial facilitation was observed in 5 of 14 cases (35.7%).

As with DRP recordings, the spatial facilitation tests led to a negative deflection in 16 trials with PADs (14 with muscle afferents, 2 with cutaneous afferents). Even though reticulospinal stimuli alone evoked PAD and no PAH, when it was combined with sensory afferents, it led to a smaller response. A decrease in sensory-evoked PAD by reticulospinal stimuli is most easily explained by reticulospinal inputs evoking presynaptic inhibition of the stimulated afferents (see Discussion).

Therefore, the results indicate that reticulospinal and sensory inputs do not converge on common presynaptic inhibitory pathways within the spinal cord, even though the experimental prep-

aration clearly had the right conditions to allow for spatial facilitation of PADs in axons and in DRP recordings.

Task-dependent modulation

Transmission in several pathways, including presynaptic inhibitory pathways, can be deeply modified when spinal networks are configured to produce rhythmic movements (Rossignol et al., 2006; Frigon, 2012). Although CPG-related changes in the transmission of sensory-evoked presynaptic inhibitory pathways have been described previously (Duenas and Rudomin, 1988; Côté and Gossard, 2003), the evidence for task-dependent modulation of presynaptic inhibition evoked by supraspinal signals during any motor task is scarce (Leblond et al., 1999). In the present study, we succeeded in comparing transmission in presynaptic inhibitory pathways activated by reticulospinal and sensory inputs at rest and during fictive locomotion or scratch. Task-dependent modulation was evaluated in 62 trials using DRPs and in 46 trials using PADs in 24 axons of 16 cats. Although fictive locomotion increased PADs and DRPs evoked by both reticulospinal and sensory inputs, the extent of the increase was larger with reticulospinal inputs. In contrast, reticulospinal- and sensory-evoked PADs and DRPs were considerably decreased during fictive scratch.

Fictive locomotion

To illustrate task-dependent modulation of PAD, Figure 4 shows changes in the amplitude of PADs during the transition from fictive locomotion to rest. Individual PAD responses (tilted 90°) are aligned to the reticulospinal stimuli (MLF, 6p, 100 μA). The first 9 stimuli were given during fictive locomotion and showed clear positive deflections (indicating PAD) in the FDHL afferent. The last 5 PADs occurred

at rest and were significantly reduced in amplitude ($p < 0.014$ for the entire episode). A similar decrease was found for DRP amplitudes ($p < 0.001$; data not shown). The DRP signal (Fig. 4, second trace) showed some waxing and waning with the locomotor cycles. These oscillations, which accompany CPG activity, are not produced by the stimuli (Dubuc et al., 1988; Gossard and Rossignol, 1990; Gossard et al., 1991), do not appear to modify sensory transmission (Gossard, 1996), and will not be considered further in this study.

Overall, we tested changes in DRP amplitude between rest and fictive locomotion in 23 trials from 6 cats. A significant change in DRP amplitude was observed in 5 of 12 trials using reticulospinal inputs with 4 of 5 showing larger DRP amplitudes during fictive locomotion compared with rest (by 35.2 ± 12.6%). We also investigated changes in PAD amplitude evoked by the same input in 13 afferents (3 SmAB, 2 FDHL, 2 LGS, 2 Sci, 2 Pl, 1 MPL, 1 PBSt) of 4 cats. Significant changes were found in 2 cases; and in both,

PAD amplitude was increased during fictive locomotion (by 39.1 ± 32.5%). DRPs evoked by sensory inputs (11 trials from 4 cats) were significantly different in 2 trials, with both showing a slightly larger amplitude during fictive locomotion (by 7.0 ± 5.1%). PADs evoked by sensory inputs in 14 afferents (3 Pl, 3 FDHL, 2 Sci, 2 LGS, 2 SmAB, 1 MPL, 1 PBSt) from 3 cats showed a significant change in only one trial, an increase of amplitude during fictive locomotion (by 10.1%), as previously reported (Côté and Gossard, 2003). Although the sample is relatively small, the locomotor-dependent increase in reticular-evoked DRPs was significantly larger than the increase in sensory-evoked DRPs.

Fictive scratch

Figure 5 shows changes in PAD amplitudes during the transition from rest to fictive scratch. Individual PAD responses (tilted 90 degrees) are aligned to the reticulospinal stimuli (RS, 6p, 18 μA). Interleaved in this episode are PADs evoked by stimulating the MPL nerve (6p, 2T) and by the combined stimuli of MPL and RS (data not shown). The amplitude of PADs and DRPs during scratch was smaller compared with rest ($p < 0.001$ for the entire episode). As in Figure 4 with fictive locomotion, there were cyclic oscillations in the DRP signal (Fig. 5, second trace) accompanying CPG activity that were not evoked by the stimuli (Côté and Gossard, 2003).

Overall, DRP amplitudes were compared at rest and during scratch in 39 trials in 8 cats, whereas PAD amplitudes were compared for 19 trials in 5 cats. The DRP amplitudes evoked by reticulospinal inputs were significantly modified during fictive scratch in 13 of 19 trials. In all 13 cases, it was a decrease (by 33.1 ± 12.4%). The same reticulospinal inputs in 6 afferents (2 LGS, 2 Sci, 1 SmAB, 1 MG) showed significant changes in PAD amplitude in 4 of 6 axons, and all were smaller during fictive scratch (by 32.1 ± 22.8%). DRPs evoked by sensory inputs (20 trials) were significantly modified in 16 trials; and in 15 of 16 of those, the amplitude was smaller during fictive scratch (by 44.8 ± 18.4%). PADs evoked by sensory inputs (13 trials in 4 cats) in 9 axons (3 Sci, 2 SmAB, 2 LGS, 1 EDL, 1 MPL) showed a significant change in 8 of 13 trials, and all showed a smaller amplitude (by 26.9 ± 16.4%) during fictive scratch compared with rest. There were no significant differences in the magnitude of scratch-induced reductions between reticular- and sensory-evoked DRPs or PADs.

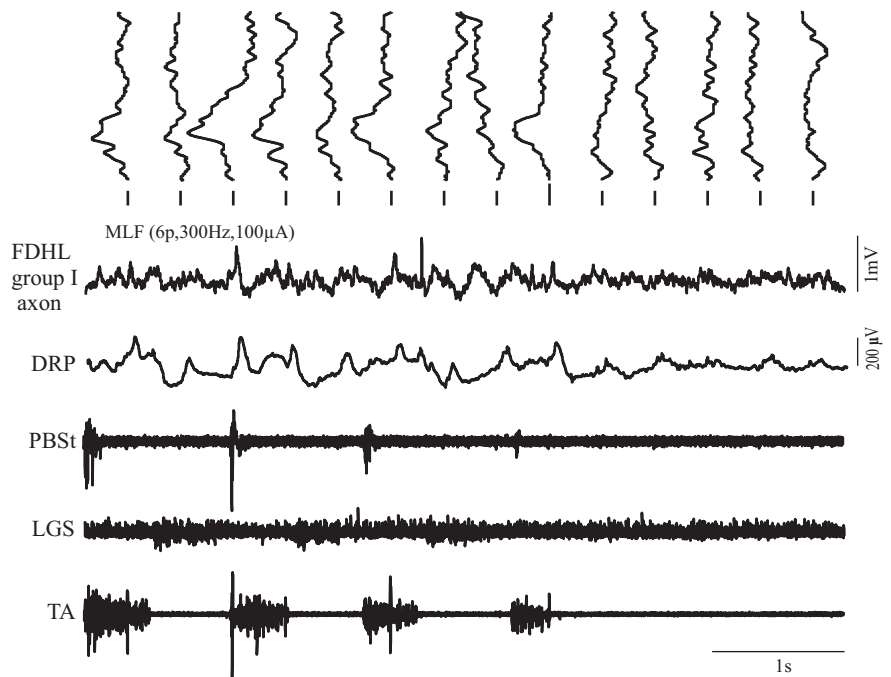## PAD amplitude increases during fictive locomotion

Figure 4. Task-dependent increase in PAD during fictive locomotion. Raw signals recorded at the end of a spontaneous episode of fictive locomotion with stimulation of reticulospinal inputs in the MLF (6 p, 300 Hz, 100 μA). Individual PAD responses (tilted 90 degrees) are aligned to the MLF stimuli. Underneath are five continuous signals: intra-axonal recording, DRP, and ENG of PBSt, LGS, and TA muscles. PADs were readily apparent during the last four locomotor cycles, but PAD amplitude decreased rapidly when the alternating ENG bursts of activity ceased.

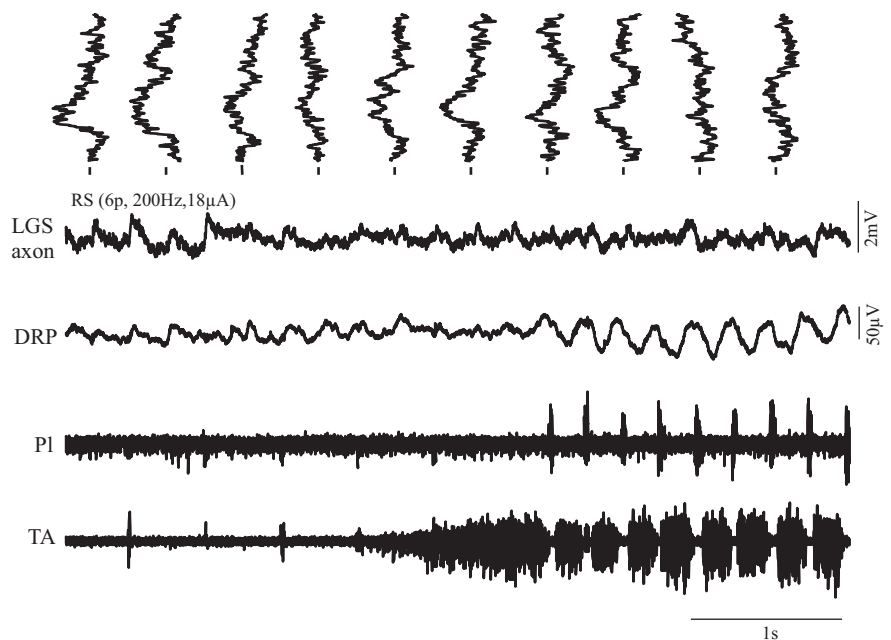## PAD amplitude decreases during fictive scratch

Figure 5. Task-dependent decrease in PAD during fictive scratch. Raw signals recorded at the beginning of an episode of fictive scratch with stimulation of RS inputs (6p, 200 Hz, 18 μA). Individual PAD responses (tilted 90 degrees) are aligned to the RS stimuli. Underneath are four continuous signals: intra-axonal recoding, DRP, and ENGs of Pl and TA muscles. PADs were readily apparent before the scratch episode and PAD amplitude decreased (and changed according to phases as described later), during the alternating ENG bursts of activity. Interleaved in this particular episode are PADs evoked by the stimulation of the MPL (6p, 2T) and by the combined stimuli of MPL and RS (data not shown).
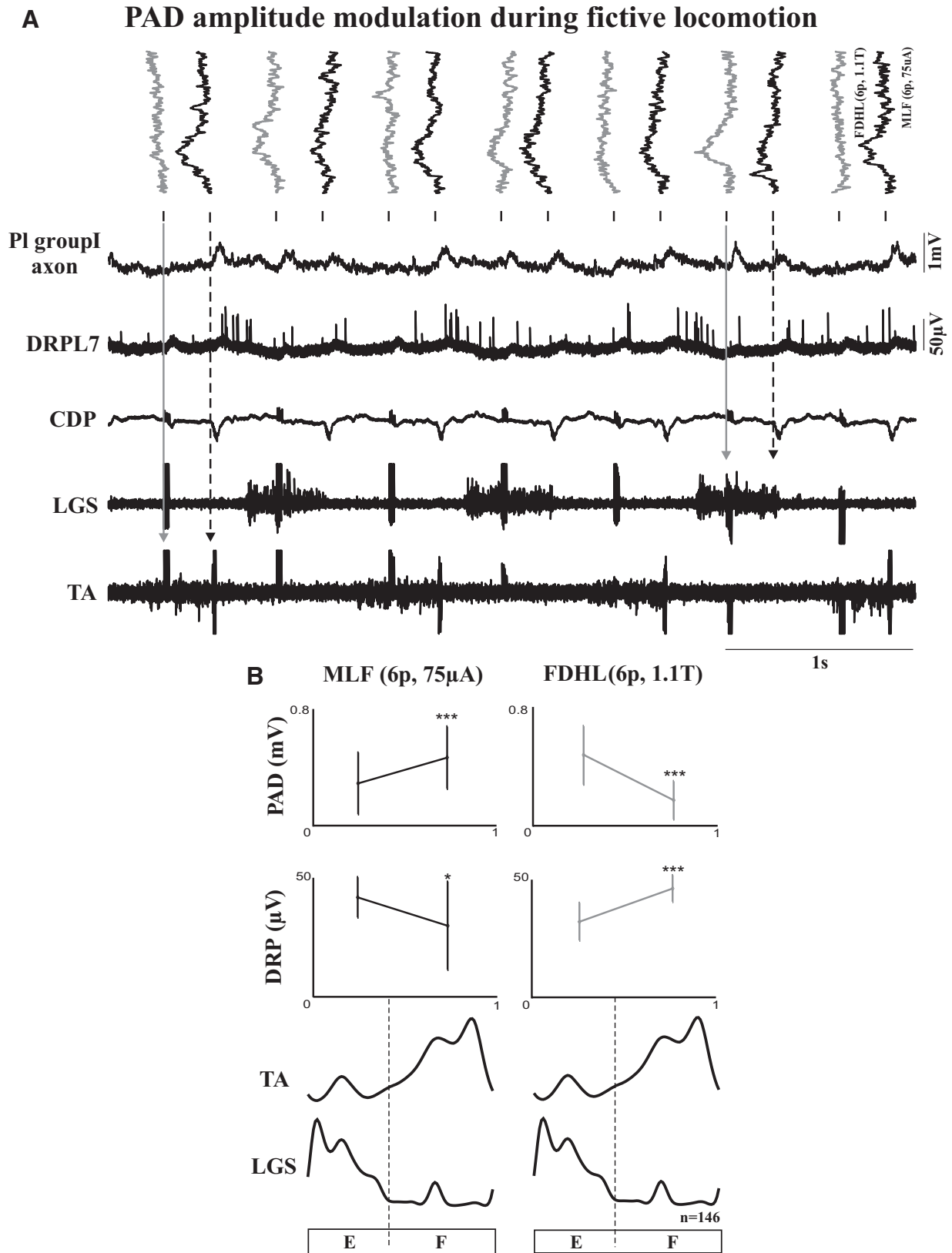
A   PAD amplitude modulation during fictive locomotion

B

Figure 6. Phase-dependent modulation of PAD during fictive locomotion. **A**, Raw signals recorded during fictive locomotion. Individual PADs (tilted 90 degrees) in a PI Group I afferent are aligned to alternating MLF (6p, 75 μA; in black) and FDHL (6p, 1.1T; in gray) stimuli. Underneath are five continuous signals: intra-axonal recording, DRP, CDP, and ENG of LGS and TA muscles. The first two downward arrows indicate PADs occurring during the TA burst or flexion phase. The last two downward arrows indicate PADs occurring during the LGS burst or extension phase. **B**, Phase plots of averaged PAD and DRP amplitude from the entire episode. The fictive step cycle is divided into the two main phases: extension and flexion. Left, Responses evoked by MLF stimuli. Right, Responses evoked by FDHL stimuli. *$p <$ 0.05. ***$p <$ 0.001.

Phase-dependent modulation

As mentioned in the Introduction, the phase-dependent modulation of presynaptic inhibition evoked by supraspinal signals is largely unknown, in contrast to presynaptic inhibition evoked by sensory feedback (Nusbaum et al., 1997; Rossignol et al., 2006). Here, we show that the amplitude of PADs and DRPs evoked by reticulospinal inputs peaked in the flexion phase during fictive locomotion and scratch. On the other hand, PAD and DRP amplitudes evoked by sensory inputs in the same conditions could peak either during the flexion or extension phases.

Fictive locomotion

Figure 6 illustrates the phase-dependent modulation of PAD evoked by reticulospinal and sensory inputs in a Group I afferent from the Pl muscle during fictive locomotion. In Figure 6A, individual PAD responses are tilted 90 degrees and aligned to alternating MLF (Fig. 6A, black; 6p, 75 μA) and FDHL (Fig. 6A, gray; 6p, 1.1T) stimuli. From the left, the PAD evoked by the first FDHL stimulation had an amplitude near zero when it occurred during the TA burst or flexion phase (Fig. 6A, gray arrow), whereas the PAD evoked by the first MLF stimulation had a large amplitude during the same phase (Fig. 6A, black dotted arrow). The PAD in the fourth sweep from the right evoked by FDHL stimulation had a large amplitude when it occurred during the LGS burst or extension phase (Fig. 6A, gray arrow), whereas the PAD next to it (third sweep from the right) evoked by MLF stimulation had a small amplitude during the same phase (Fig. 6A, black dotted arrow).

PAD and DRP amplitudes evoked by MLF and FDHL stimulation were averaged for the entire episode and divided into extension and flexion phases (Fig. 6B). PAD amplitudes evoked by MLF stimuli were significantly increased during flexion ($p < 0.001$), whereas DRP amplitudes were significantly increased in extension ($p < 0.026$). In contrast, PAD amplitudes evoked by FDHL stimuli were significantly smaller during flexion ($p < 0.001$), whereas DRP amplitudes were significantly smaller in extension ($p < 0.001$). Thus, in this Pl Group I afferent, the phase-dependent modulation was clearly different for PADs evoked by reticulospinal and sensory inputs. In this example, PAD and DRP showed an opposite phase-dependent pattern. That is not surprising, considering that the DRP is a recording of PADs from an unknown mix of afferents (of all calibers), some with maximal PAD in flexion and some in extension; the resulting DRP could be maximal in either phase depending on the mix (e.g., Gossard et al., 1990).

Overall, DRPs evoked by reticulospinal inputs (28 trials in 13 cats) showed significant phase-dependent modulation in 15 trials. In 14 of 15 trials, DRP amplitudes were significantly larger during the flexion phase compared with the extension phase (by $26.6 \pm 17.4\%$). PADs evoked by reticulospinal inputs (21 trials in 7 cats) were studied in 19 axons (3 Sci, 4 SmAB, 3 Pl, 3 LGS, 2 MPL, 2 FDHL, 1 EDL, 1 PBSt). In 3 of 21 trials, there was a significant phase-dependent modulation; and in all, PAD amplitudes were greater during the flexion phase (by $25.0 \pm 13.3\%$). Therefore, the most common significant change in amplitude for DRPs or PADs evoked by reticulospinal inputs was an increase during flexion.

On the other hand, DRPs evoked by sensory inputs (31 trials in 7 cats) showed a significant phase-dependent modulation in 23 trials and the amplitude was larger during flexion in 8 of 23 trials (by $22.5 \pm 14.1\%$) or during extension in 15 of 23 trials (by $28.5 \pm 35.8\%$). PADs evoked by sensory inputs (30 trials in 7 cats) in 22 axons (5 Sci, 4 LGS, 4 SmAB, 3 Pl, 3MPL, 1 FDHL, 1 EDL, 1 PBSt) showed significant phase-dependent modulation in 11 trials. In 6 of 11 trials, PAD amplitudes were larger in extension (by $43.6 \pm 42.0\%$), whereas in the other 5 of 11 trials, amplitudes were larger during flexion (by $16.9 \pm 9.6\%$). That sensory-evoked PAD amplitudes peaked in different phases of the fictive locomotion cycle is consistent with previous reports (Ménard et al., 1999, 2002).

Fictive scratch

The phase-dependent modulation of presynaptic inhibition is more difficult to evaluate during fictive scratch because episodes are relatively short and the duration of the extension phase is very brief. Figure 7 shows the only example with significant modulation in amplitude for all PADs and DRPs. PADs evoked by reticulospinal inputs (RS, Fig. 7, black; 6p, 100 μA) had a smaller amplitude during extension (Fig. 7, first black dotted arrow) compared with PADs evoked during flexion (Fig. 7, second black dotted arrow at the end of TA burst). The PAD evoked by PBSt (Fig. 7, gray; 6p, 1.7T) had a smaller amplitude during flexion (Fig. 7, first gray arrow) compared with extension (Fig. 7, second gray arrow) where it triggered an action potential.

PAD and DRP amplitudes evoked by reticulospinal and PBSt stimulation were averaged for the entire episode and divided into flexion and extension (Fig. 7B). Both PADs and DRPs evoked by reticulospinal stimuli were significantly larger during the flexion phase. On the other hand, PAD and DRP amplitudes evoked by PBSt stimuli were significantly larger during extension.

Overall, we analyzed DRPs evoked by reticulospinal inputs in 12 trials from 7 cats. There was a significant phase-dependent modulation in 9 of 12 trials; and in all, DRP amplitudes were larger during flexion (by $58.4 \pm 27.3\%$). PADs evoked by the same input in 4 axons (2 Sci, 1 LGS, and 1 MG) from 4 cats showed significant phase-dependent modulation in only 1 of 4 trials, with an increase in flexion (by 49.8%). Sensory-evoked DRPs (9 trials in 5 cats) showed significant phase-dependent modulation in 6 of 9 trials, with larger amplitudes during flexion in 5 of 6 trials (by $68.0 \pm 23.7\%$) and during extension in the other trial (by 38.8%). Sensory-evoked PADs (5 trials in 5 cats) in 5 axons (3 Sci, 1 LGS, and 1 MG) showed significant phase-dependent modulation in 2 of 5 trials with larger amplitudes during flexion in one trial (by 14.7%) and during extension in the other (by 61.8%). Thus, 16 of 18 significant phase-dependent changes in RS-evoked responses showed maximal amplitude in flexion.

Fictive locomotion and scratch

In two cats, the modulation of DRPs was compared during both fictive locomotion and scratch, confirming that changes were dependent on the task or inputs and not on the state of individual cats. In one cat, DRPs evoked by reticulospinal inputs (RS, 6p, 75 μA) during fictive scratch were significantly larger during flexion compared with the extension phase (by 90.1%, $p < 0.003$). However, during fictive locomotion, there was no significant phase-dependent modulation. Stimulation of PBSt (6p, 2T) evoked significantly larger DRPs during the flexion phase of fictive locomotion ($p < 0.001$, by 42.4%) and fictive scratch ($p < 0.008$, by 81.1%) compared with extension. In the other cat, DRPs evoked by reticulospinal inputs (RS, 6p, 100 μA) were significantly larger during the flexion phase of both fictive locomotion ($p < 0.02$, by 2.4%) and scratch ($p < 0.001$, by 5.9%) compared with the extension phase.
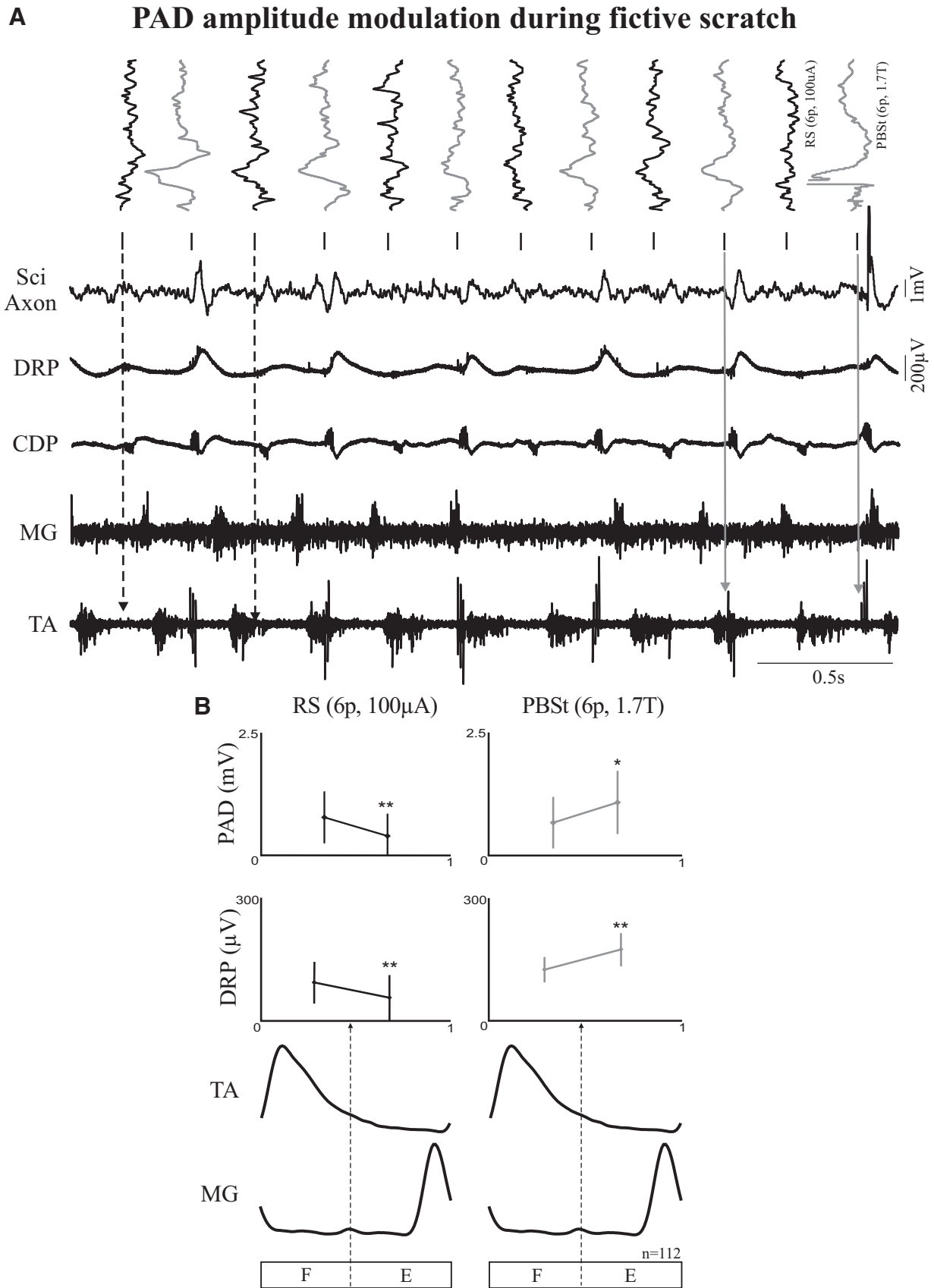
PAD amplitude modulation during fictive scratch

Figure 7. Phase-dependent modulation of PAD during fictive scratch. **A**, Similar outline as in Figure 6. PADs were evoked by stimulating the reticular formation (RS, 6p, 100 μA; in gray) interleaved with stimuli of the nerves to PBSt (6p, 1.7T; in black). The five continuous signals are as follows: intra-axonal recording (Sci axon), DRP, CDP, and ENG of MG and TA muscles. The black dotted arrows indicate PADs evoked by RS stimuli, and the gray downward arrows indicate PADs evoked by PBSt stimuli occurring in different phases. **B**, Phase plots of averaged PADs and DRPs amplitude evoked by RS inputs (left) and PBSt inputs (right). *$p < 0.05$. **$p < 0.01$.

Discussion

Evidence for separate presynaptic inhibitory pathways to primary afferents

Spatial facilitation could be obtained when two muscle afferent inputs were combined, indicating that interneuronal convergence was possible in our preparation (Brink et al., 1984). However, spatial facilitation was extremely rare when inputs from the reticular formation and sensory nerves were combined, indicating that these two inputs independently control presynaptic inhibition. Spatial facilitation can disclose convergence on common interneurons whether pathways are disynaptic or polysynaptic (Lundberg et al., 1975; Schomburg et al., 1999; Leblond et al., 2000; Stecina and Jankowska, 2007; Alstermark and Isa, 2012). In disynaptic pathways, the two afferents make monosynaptic contacts on common interneurons; whereas in polysynaptic pathways, we cannot determine whether afferents make monosynaptic or oligosynaptic contacts on common interneurons. A diagram of PAD circuitry based on our findings is illustrated in Figure 8A (left). Sensory afferents and reticulospinal axons project to parallel PAD pathways contacting the same afferent terminal. The projection of reticulospinal axon on the second interneuron in the chain is based on results from Rudomin's group where PAD interneurons were directly activated by intraspinal stimulation in anesthetized cats (Rudomin et al., 1983, 1986; Enriquez et al., 1996b).

The phase-dependent modulation of DRPs and PADs activated by reticulospinal and sensory inputs during fictive locomotion is also consistent with separate presynaptic inhibitory pathways. DRP and PAD amplitudes evoked by reticulospinal inputs were increased during the flexion phase in the vast majority of cases, whereas sensory-evoked DRPs and PADs showed maximal amplitude in either flexion or extension phases. Different CPG-related modulation patterns argue strongly for separate interneuronal pathways (Burke, 1999). This is illustrated in Figure 8B. During flexion, the CPG increases the excitability of parallel, albeit separate, PAD pathways. During extension, the CPG increases only the excitability of PAD pathways contacted by sensory afferents. During fictive scratch, DRPs or PADs from either source had a maximal amplitude predominantly in flexion. The simplest explanation is that the separate PAD pathways received the same phasic drive from the CPG for scratch during flexion only, as illustrated in Figure 8C.

Tests for spatial facilitation between reticulospinal and sensory inputs also showed negative deflections for DRPs (21 of 45 trials) and PADs (16 of 58 trials). That could be the result of occlusion (Carpenter and Rudomin, 1973; Jankowska, 1975). Occlusion occurs when combined inputs converging on the same interneurons are stimulated with too much intensity. The first stimulus recruits so many interneurons that the other stimulus cannot produce additional recruitment. Thus, when the sum of individual responses is subtracted from the combined response, the result is a negative deflection. Occlusion can be considered as an additional indication of interneuronal convergence (Jankowska, 1975; Brink et al., 1984). In one case of spatial facilitation between two sensory inputs, we combined higher-intensity stimuli and found, as expected, a negative deflection indicating occlusion. In the same axon, the combination of reticulospinal and sensory inputs led to a flat line whether they were stimulated with low or high intensities, indicating no occlusion. This exemplifies that negative deflections without spatial facilitation cannot be explained by convergence on common interneurons. A simpler explanation is PAD evoked in the stimulated
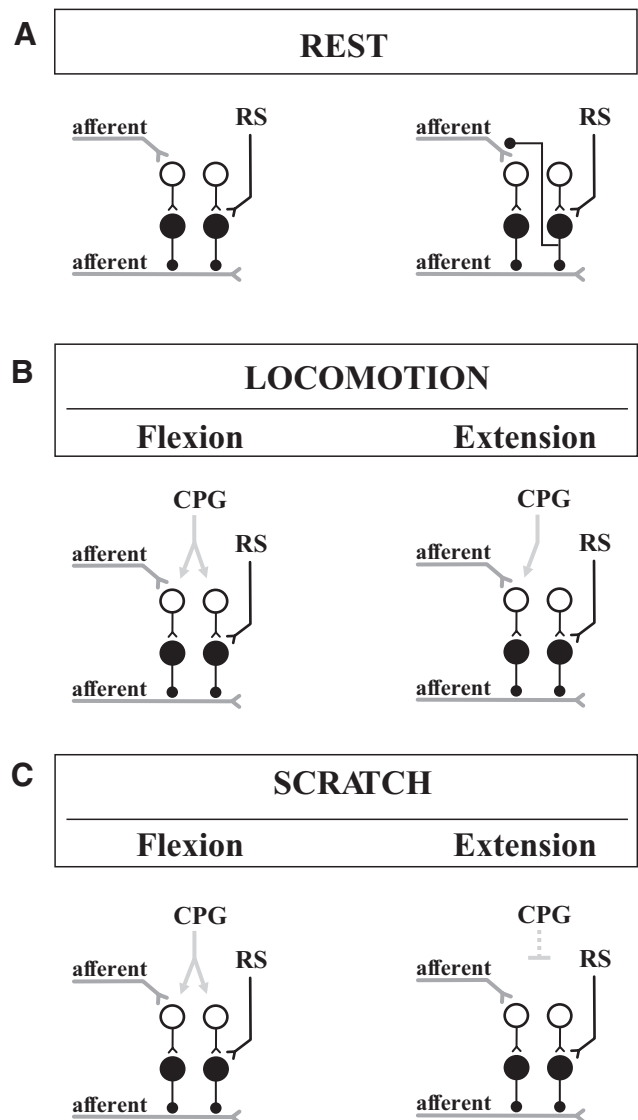

Figure 8. Diagrams of PAD circuitry. ***A***, At rest, there was an absence of spatial facilitation in the vast majority of cases when we combined reticulospinal and sensory inputs. Left, The PAD pathways activated by these two systems are thus separate and meet at the level of the afferent terminal. In some cases, the combination led to a smaller PAD than the sum of individual PADs. This is most easily explained by the reticulospinal inputs mediating a presynaptic inhibition of the stimulated sensory afferents. Right, Diagram showing an axonal branch from the GABAergic last-order interneuron making contact with the terminals of the stimulated afferents. ***B***, The vast majority of PADs evoked by reticulospinal inputs during fictive locomotion had maximal amplitude during flexion, whereas PADs evoked by sensory inputs had maximal amplitude in either phase. The CPG for locomotion thus increases the excitability of the two separate PAD pathways during flexion, in the left diagram, but increases the excitability of PAD pathways stimulated by sensory afferents only during extension, in the right diagram. ***C***, The majority of PADs evoked by reticulospinal and sensory inputs had a maximal amplitude during flexion during fictive scratch. The CPG for scratch thus increases the excitability of the two separate PAD pathways during flexion, in the left diagram, but not during extension, in the right diagram.

afferents (Burke, 1999). This is illustrated in Figure 8A (right) whereby an axonal branch from the last-order PAD interneuron makes contact with the afferent being stimulated. We suggest that RS stimulation evoked presynaptic inhibition in some of the stimulated afferents, thus resulting in a smaller PAD. Evidently, this was not seen in all stimulated afferents, as different types of axons respond with different amplitudes of PAD (or no PAD) to RS stimulation. As sensory inputs do not evoke presynaptic inhibition in descending terminals from supraspinal structures (Ru-

domin and Jankowska, 1981; Rudomin et al., 1981; Curtis and Malik, 1985), PAD from reticulospinal inputs would not be modified.

Task-dependent modulation of presynaptic inhibition

Presynaptic inhibitory pathways activated by reticulospinal or peripheral sensory inputs showed similar patterns of task-dependent modulation during fictive locomotion and scratch. For instance, PAD transmission activated by both sources was significantly increased during fictive locomotion. Thus, the locomotor CPG increases the overall excitability of several separate PAD pathways, enhancing presynaptic inhibition. In contrast, PAD transmission activated by both sources was decreased overall during fictive scratch. One could argue (as above) that the stimulated sensory afferents were themselves subjected to strong PAD during scratch and that the evoked PADs were therefore decreased. However, reticulospinal terminals, which are apparently devoid of PAD, also evoked responses with decreased amplitude during fictive scratch. Therefore, our results are consistent with an overall reduction in the transmission of PAD pathways during scratch (Côté and Gossard, 2003). The scratch CPG thus decreases the overall excitability of several PAD pathways and limits presynaptic inhibition.

Phase-dependent modulation of presynaptic inhibition

Phase-dependent changes in PAD transmission activated by reticulospinal inputs showed an increase during the flexion phase of fictive locomotion, whereas sensory-evoked PADs could be maximal during flexion or extension. This finding and other reports (Brink et al., 1984; Leblond et al., 1999; Ménard et al., 1999) indicate that the locomotor CPG may project to several distinct PAD pathways activated by different descending and sensory sources. During fictive scratch, PAD transmission for reticulospinal inputs and for the majority of sensory-evoked responses was maximal in flexion. This may be the result partly of the specific structure of the scratch cycle where the duration of the flexion phase occupies most of the cycle (Kuhta and Smith, 1990; Frigon and Gossard, 2010), which could underestimate PAD changes during extension in our experimental conditions.

Why the CPGs for locomotion and scratch selectively enhance presynaptic inhibition induced by reticulospinal inputs during flexion remains unclear, considering that the actions of reticulospinal inputs are not restricted to flexors or the flexion phase. For example, stimulation of reticular neurons during stepping can modify the amplitude and timing of ongoing bursts of activity in flexors and extensors in the forelimbs and hindlimbs (Orlovsky, 1972; Drew, 1991; Floeter et al., 1993; Leblond et al., 2000).

One explanation may be the different biomechanical demands related to the two phases of the cycle. During stepping, the stance phase is characterized by varying loads and pressures during ground contact, whereas the swing phase appears as a recurring unperturbed movement whose duration varies little with speed (Gossard et al., 2011). A similar situation is seen during scratch where load is put on the toes and claws during the extension phase when the limb encounters the irritated skin, whereas the flexion phase (or return stroke) occurs in the air without contact. One could speculate that commands from the reticular formation during flexion are accompanied by descending presynaptic inhibitory patterns to filter out the predictable reafference during the swing phase or return stroke (Kuhta and Smith, 1990; Rossignol et al., 2006). On the other hand, less presynaptic inhibition during extension may facilitate the transmission of sensory information related to load or to adjust postural tone during the stance phase of locomotion (Leblond et al., 2000) while adjusting the contact force and duration on the irritated skin area during scratch (Kuhta and Smith, 1990).

State-dependent organization of presynaptic inhibition

Another finding indicates a state-dependent organization of PAD pathways. The prevalence of PADs in our sample of Group I afferents (25 of 26 Group I axons), instead of PAH (1 of 26), evoked by reticulospinal inputs was much higher than reported in anesthetized cats where reticulospinal inputs evoked PAH in 52% of Group IAs and in 89% of Group IBs (Rudomin et al., 1986; Enriquez et al., 1996b). It is unlikely that the random penetrations of the micropipette in our experiments always missed the afferents with PAH. We thus think that there was a state-dependent change in the balance between inhibitory and excitatory contacts from reticulospinal afferents to PAD interneurons in the decerebrate cat favoring excitation. Other reports suggest that the balance between excitatory and inhibitory connections from brainstem to spinal PAD pathways may be continuously adjusted and plastic. Indeed, weeks after crushing the medial gastrocnemius nerve, the reticular formation was found to evoke PAD in all IA-regenerated afferents in anesthetized cats (Enriquez et al., 1996a).

Presynaptic inhibition and movements in humans

Overall, our evidence indicates that presynaptic inhibitory pathways activated by the reticular formation can be independent from those activated by peripheral sensory feedback. Task-dependent results indicate that the excitability of both pathways may be increased (i.e., locomotion) or decreased (i.e., scratch) in parallel, whereas phase-dependent results indicate that they can be driven in phase or in alternation. Such an arrangement may allow the reticular formation to program different movements, at appropriate phases of a movement, with specific presynaptic inhibitory patterns independent of sensory feedback. Consequently, testing PAD pathways by using sensory volleys during movements and posture in healthy or neurologically injured humans may monitor only part of the ongoing presynaptic inhibition (Butchart et al., 1993; Calancie et al., 1993; Earles et al., 2001; Bove et al., 2003; Kitano et al., 2009; Roche et al., 2011). Sensory stimulation studies should be complemented with other techniques, such as changes in heteronymous Ia facilitation (Hultborn et al., 1987a, 1987b) to evaluate the overall level of ongoing presynaptic inhibition (Faist et al., 1994, 1996; Morita et al., 1995, 2000; Baudry et al., 2011).

References

Alstermark B, Isa T (2012) Circuits for skilled reaching and grasping. Annu Rev Neurosci 35:559–578. CrossRef Medline

Andersen P, Eccles JC, Sears TA (1964) Cortically evoke depolarization of primary afferent fibers in the spinal cord. J Neurophysiol 27:63–77. Medline

Baudry S, Maerz AH, Gould JR, Enoka RM (2011) Task- and time-dependent modulation of Ia presynaptic inhibition during fatiguing contractions performed by humans. J Neurophysiol 106:265–273. CrossRef Medline

Bove M, Nardone A, Schieppati M (2003) Effects of leg muscle tendon vibration on group Ia and group II reflex responses to stance perturbation in humans. J Physiol 550:617–630. CrossRef Medline

Brink E, Jankowska E, Skoog B (1984) Convergence onto interneurons subserving primary afferent depolarization of group I afferents. J Neurophysiol 51:432–449. Medline

Burke RE (1999) The use of state-dependent modulation of spinal reflexes

as a tool to investigate the organization of spinal interneurons. Exp Brain Res 128:263–277. CrossRef Medline

Butchart P, Farquhar R, Part NJ, Roberts RC (1993) The effect of age and voluntary contraction on presynaptic inhibition of soleus muscle Ia afferent terminals in man. Exp Physiol 78:235–242. Medline

Cabaj A, Stecina K, Jankowska E (2006) Same spinal interneurons mediate reflex actions of group Ib and group II afferents and crossed reticulospinal actions. J Neurophysiol 95:3911–3922. CrossRef Medline

Calancie B, Broton JG, Klose KJ, Traad M, Difini J, Ayyar DR (1993) Evidence that alterations in presynaptic inhibition contribute to segmental hypo- and hyperexcitability after spinal cord injury in man. Electroencephalogr Clin Neurophysiol 89:177–186. CrossRef Medline

Carpenter DO, Rudomin P (1973) The organization of primary afferent depolarization in the isolated spinal cord of the frog. J Physiol 229:471–493. Medline

Carpenter D, Engberg I, Lundberg A (1966) Primary afferent depolarization evoked from the brain stem and the cerebellum. Arch Ital Biol 104:73–85. Medline

Cattaert D, El Manira A (1999) Shunting versus inactivation: analysis of presynaptic inhibitory mechanisms in primary afferents of the crayfish. J Neurosci 19:6079–6089. Medline

Cook WA Jr, Cangiano A, Pompeiano O (1969) Vestibular control of transmission in primary afferents to the lumbar spinal cord. Arch Ital Biol 107:296–320. Medline

Côté MP, Gossard JP (2003) Task-dependent presynaptic inhibition. J Neurosci 23:1886–1893. Medline

Curtis DR, Malik R (1985) The differential effects of baclofen on segmental and descending excitation of spinal interneurones in the cat. Exp Brain Res 58:333–337. Medline

Deliagnina TG, Feldman AG, Gelfand IM, Orlovsky GN (1975) On the role of central program and afferent inflow in the control of scratching movements in the cat. Brain Res 100:297–313. CrossRef Medline

Drew T (1991) Functional organization within the medullary reticular formation of the intact unanesthetized cat: III. Microstimulation during locomotion. J Neurophysiol 66:919–938. Medline

Dubuc R, Cabelguen JM, Rossignol S (1988) Rhythmic fluctuations of dorsal root potentials and antidromic discharges of single primary afferents during fictive locomotion in the cat. J Neurophysiol 60:2014–2036. Medline

Dueñas SH, Rudomin P (1988) Excitability changes of ankle extensor group 1a and 1b fibers during fictive locomotion in the cat. Exp Brain Res 70:15–25. Medline

Earles D, Vardaxis V, Koceja D (2001) Regulation of motor output between young and elderly subjects. Clin Neurophysiol 112:1273–1279. CrossRef Medline

Eccles JC, Schmidt RF, Willis WD (1962) Presynaptic inhibition of the spinal monosynaptic reflex pathway. J Physiol 161:282–297. Medline

Eccles JC, Schmidt RF, Willis WD (1963) Pharmacological studies on presynaptic inhibition. J Physiol 168:500–530. Medline

Enríquez M, Jiménez I, Rudomin P (1996a) Changes in PAD patterns of group I muscle afferents after a peripheral nerve crush. Exp Brain Res 107:405–420. Medline

Enríquez M, Jiménez I, Rudomin P (1996b) Segmental and supraspinal control of synaptic effectiveness of functionally identified muscle afferents in the cat. Exp Brain Res 107:391–404. Medline

Faist M, Mazevet D, Dietz V, Pierrot-Deseilligny E (1994) A quantitative assessment of presynaptic inhibition of Ia afferents in spastics: differences in hemiplegics and paraplegics. Brain 117:1449–1455. CrossRef Medline

Faist M, Dietz V, Pierrot-Deseilligny E (1996) Modulation, probably presynaptic in origin, of monosynaptic Ia excitation during human gait. Exp Brain Res 109:441–449. Medline

Feldberg W, Fleischhauer K (1960) Scratching movements evoked by drugs applied to the upper cervical cord. J Physiol 151:502–517. Medline

Floeter MK, Sholomenko GN, Gossard JP, Burke RE (1993) Disynaptic excitation from the medial longitudinal fasciculus to lumbosacral motoneurons: modulation by repetitive activation, descending pathways, and locomotion. Exp Brain Res 92:407–419. Medline

Frigon A (2012) Central pattern generators of the mammalian spinal cord. Neuroscientist 18:56–69. CrossRef Medline

Frigon A, Gossard JP (2010) Evidence for specialized rhythm-generating mechanisms in the adult mammalian spinal cord. J Neurosci 30:7061–7071. CrossRef Medline

Frigon A, Sirois J, Gossard JP (2010) Effects of ankle and hip muscle afferent inputs on rhythm generation during fictive locomotion. J Neurophysiol 103:1591–1605. CrossRef Medline

Gossard JP (1996) Control of transmission in muscle group IA afferents during fictive locomotion in the cat. J Neurophysiol 76:4104–4112. Medline

Gossard JP, Rossignol S (1990) Phase-dependent modulation of dorsal root potentials evoked by peripheral nerve stimulation during fictive locomotion in the cat. Brain Res 537:1–13. CrossRef Medline

Gossard JP, Cabelguen JM, Rossignol S (1989) Intra-axonal recordings of cutaneous primary afferents during fictive locomotion in the cat. J Neurophysiol 62:1177–1188. Medline

Gossard JP, Cabelguen JM, Rossignol S (1990) Phase-dependent modulation of primary afferent depolarization in single cutaneous primary afferents evoked by peripheral stimulation during fictive locomotion in the cat. Brain Res 537:14–23. CrossRef Medline

Gossard JP, Cabelguen JM, Rossignol S (1991) An intracellular study of muscle primary afferents during fictive locomotion in the cat. J Neurophysiol 65:914–926. Medline

Gossard JP, Floeter MK, Degtyarenko AM, Simon ES, Burke RE (1996) Disynaptic vestibulospinal and reticulospinal excitation in cat lumbosacral motoneurons: modulation during fictive locomotion. Exp Brain Res 109:277–288. Medline

Gossard JP, Sirois J, Noué P, Côté MP, Ménard A, Leblond H, Frigon A (2011) The spinal generation of phases and cycle duration. Prog Brain Res 188:15–29. CrossRef Medline

Hongo T, Jankowska E, Lundberg A (1972) The rubrospinal tract: III. Effects on primary afferent terminals. Exp Brain Res 15:39–53. Medline

Hughes DI, Mackie M, Nagy GG, Riddell JS, Maxwell DJ, Szabó G, Erdélyi F, Veress G, Szucs P, Antal M, Todd AJ (2005) P boutons in lamina IX of the rodent spinal cord express high levels of glutamic acid decarboxylase-65 and originate from cells in deep medial dorsal horn. Proc Natl Acad Sci U S A 102:9038–9043. CrossRef Medline

Hultborn H, Meunier S, Morin C, Pierrot-Deseilligny E (1987a) Assessing changes in presynaptic inhibition of Ia fibres: a study in man and the cat. J Physiol 389:729–756. Medline

Hultborn H, Meunier S, Pierrot-Deseilligny E, Shindo M (1987b) Changes in presynaptic inhibition of Ia fibres at the onset of voluntary contraction in man. J Physiol 389:757–772. Medline

Jankowska E (1975) Identification of interneurons interposed in different spinal reflex pathways. In: Golgi Centennial Symposium, Proceedings (Santini M, ed), pp 235–246. New York: Raven.

Kitano K, Tsuruike M, Robertson CT, Kocejal DM (2009) Effects of a complex balance task on soleus H-reflex and presynaptic inhibition in humans. Electroencephalogr Clin Neurophysiol 49:235–243. Medline

Kuhta PC, Smith JL (1990) Scratch responses in normal cats: hindlimb kinematics and muscle synergies. J Neurophysiol 64:1653–1667. Medline

Leblond H, Ménard A, Gossard JP (1999) Modulation of dorsal root potentials evoked bu supraspinal stimulation during fictive locomotion in the cat. Soc Neurosci Abstr 25:49.6.

Leblond H, Ménard A, Gossard JP (2000) Bulbospinal control of spinal cord pathways generating locomotor extensor activities in the cat. J Physiol 525:225–240. CrossRef Medline

Lundberg A, Malmgren K, Schomburg ED (1975) Convergence from Ib, cutaneous and joint afferents in reflex pathways to motoneurones. Brain Res 87:81–84. CrossRef Medline

Matthews PBC (1972) Mammalian muscle receptors and their central actions. London: Edward Arnold.

Ménard A, Leblond H, Gossard JP (1999) The modulation of presynaptic inhibition in single muscle primary afferents during fictive locomotion in the cat. J Neurosci 19:391–400. Medline

Ménard A, Leblond H, Gossard JP (2002) Sensory integration in presynaptic inhibitory pathways during fictive locomotion in the cat. J Neurophysiol 88:163–171. Medline

Meunier S, Pierrot-Deseilligny E (1998) Cortical control of presynaptic inhibition of Ia afferents in humans. Exp Brain Res 119:415–426. CrossRef Medline

Morita H, Shindo M, Yanagawa S, Yoshida T, Momoi H, Yanagisawa N (1995) Progressive decerase in heteronymous monosynaptic IA facilitation with human ageing. Exp Brain Res 104:167–170. Medline

Morita H, Shindo M, Ikeda SI, Yanagisawa N (2000) Decrease in presynap-

tic inhibition on heteronymous monosynaptic IA terminals in patients with Parkinson's disease. Move Disord 15:830–834. CrossRef Medline

Nicoll RA, Alger BE (1979) Presynaptic inhibition: transmitter and ionic mechanisms. Int Rev Neurobiol 21:217–258. CrossRef Medline

Nusbaum MP, El Manira A, Gossard JP, Rossignol S (1997) Presynaptic mechanisms during rhythmic activity in vertebrates and invertebrates. In: Neurons, networks, and motor behavior (Stein PSG, Grillner S, Selverston AI, Stuart DG, eds), pp 237–253. London: MIT.

Orlovsky GN (1972) The effect of different descending systems on flexor and extensor activity during locomotion. Brain Res 40:359–371. CrossRef Medline

Perreault MC, Shefchyk SJ, Jiménez I, McCrea DA (1999) Depression of muscle and cutaneous afferent-evoked monosynaptic field potentials during fictive locomotion in the cat. J Physiol 521:691–703. CrossRef Medline

Robertson CT, Kitano K, Koceja DM, Riley ZA (2012) Temporal depression of the soleus H-reflex during passive stretch. Exp Brain Res 219:217–225. CrossRef Medline

Roche N, Bussel B, Maier MA, Katz R, Lindberg P (2011) Impact of precision grip tasks on cervical spinal network excitability in humans. J Physiol 589:3545–3558. CrossRef Medline

Rossignol S, Dubuc R, Gossard JP (2006) Dynamic sensorimotor interactions in locomotion. Physiol Rev 86:89–154. CrossRef Medline

Rudomin P, Jankowska E (1981) Presynaptic depolarization of terminals of rubrospinal tract fibers in intermediate nucleus of cat spinal cord. J Neurophysiol 46:517–531. Medline

Rudomin P, Schmidt RF (1999) Presynaptic inhibition in the vertebrate spinal cord revisited. Exp Brain Res 129:1–37. CrossRef Medline

Rudomin P, Engberg I, Jiménez I (1981) Mechanisms involved in presynaptic depolarization of group I and rubrospinal fibers in cat spinal cord. J Neurophysiol 46:532–548. Medline

Rudomin P, Jiménez I, Solodkin M, Dueñas S (1983) Sites of action of segmental and descending control of transmission on pathways mediating PAD of Ia and Ib afferent fibers in cat spinal cord. J Neurophysiol 50:743–769. Medline

Rudomin P, Solodkin M, Jiménez I (1986) PAD and PAH response patterns of group Ia and Ib fibers to cutaneous and descending inputs in the cat spinal cord. J Neurophysiol 56:987–1006. Medline

Schomburg ED, Steffens H, Kniffki KD (1999) Contribution of group III and IV muscle afferents to multisensorial spinal motor control in cats. Neurosci Res 33:195–206. CrossRef Medline

Simonsen EB, Dyhre-Poulsen P (1999) Amplitude of the human soleus H reflex during walking and running. J Physiol 515:929–939. CrossRef Medline

Stecina K, Jankowska E (2007) Uncrossed actions of feline corticospinal tract neurones on hindlimb motoneurones evoked via ipsilaterally descending pathways. J Physiol 580:119–132. CrossRef Medline

Wolf H, Burrows M (1995) Proprioceptive sensory neurons of a locust leg receive rhythmic presynaptic inhibition during walking. J Neurosci 15:5623–5636. Medline